LA-7937-PR
Progress Report

Thermochemical Processes for Hydrogen Production

October 1, 1978—March 31, 1979

University of California

LOS ALAMOS SCIENTIFIC LABORATORY
Post Office Box 1663 Los Alamos, New Mexico 87545

Previous reports in this series, unclassified, are LA-5731-PR, LA-6970-PR, LA-7234-PR, and LA-7629-PR.

Work supported by the US Department of Energy, Division of Energy Storage Systems.

LA-7937-PR
Progress Report
UC-94d
Issued: September 1979

Thermochemical Processes for Hydrogen Production

October 1, 1978—March 31, 1979

Compiled by

Kenneth E. Cox

Person in Charge:	**M. G. Bowman**
Principal Investigators:	**K. E. Cox**
	J. D. Farr
Work Performed by:	**K. E. Cox**
	W. M. Jones
	C. L. Peterson

THERMOCHEMICAL PROCESSES FOR HYDROGEN PRODUCTION

OCTOBER 1, 1978—MARCH 31, 1979

Compiled by

Kenneth E. Cox

Person in Charge:	M. G. Bowman
Principal Investigators:	K. E. Cox and J. D. Farr
Work Performed by:	K. E. Cox
	W. M. Jones
	C. L. Peterson

ABSTRACT

The work described in this report was accomplished during the period October 1, 1978-March 31, 1979, on a DOE-sponsored program aimed at developing efficient and economic thermochemical cycles for hydrogen production from a variety of high-temperature energy sources such as fusion, fission, and solar energy.

Most of the effort was applied to a study of the Los Alamos Scientific Laboratory (LASL) hybrid bismuth sulfate cycle. The work included a conceptual design of the cycle, made to obtain performance parameters, and experimental work done to verify the design conditions. Key findings were:

- A 50% efficiency was obtained when an improved cycle design was coupled to a fusion energy source at 1500 K. The improved design was based on a reduced endothermic requirement for $Bi_2O_3 \cdot 2SO_3$ decomposition and a lower voltage for SO_2 electrolysis that should result at lower acid concentrations.
- Experimental results showed an endothermic heat requirement of +172 kJ/mol for the decomposition of $Bi_2O_3 \cdot 2SO_3$ to $Bi_2O_3 \cdot SO_3$ and SO_3.
- Reaction times for bismuth sulfate decomposition were determined as a function of temperature. At 1240 K, < 1.5 min were required for the first two stages of decomposition from $Bi_2O_3 \cdot 3SO_3$ to $Bi_2O_3 \cdot SO_3$.
- In tests made to determine the feasibility of decomposing $Bi_2O_3 \cdot 2SO_3$ in a fluidized bed, the solid particles agglomerated when heated. Solid particles suitable for fluidization will be sought through new approaches.

I. FUSION SYNFUEL (HYDROGEN) DESIGN STUDY

A. Introduction

Thermochemical cycles for hydrogen production have been investigated at the Los Alamos Scientific Laboratory (LASL) since the early 1970s. The work consists of experimental and engineering research to define cycles that can be coupled feasibly to high-temperature heat sources for water-splitting to produce hydrogen and oxygen. Process development is sponsored by DOE's Division of Energy Storage Systems (STOR). In recent months, our efforts were concentrated on the development of a thermochemical cycle compatible with a 1500 K heat source derived from a conceptual fusion driver. The major task of this study is to define nonelectrical fusion energy applications. Chief among these applications is the production of synfuel (hydrogen) from fusion power. The study is a joint effort involving thermochemical process development (under STOR) and design and engineering systems for extracting fusion heat (under the Office of Magnetic Fusion Energy). This report describes progress in process design related to the thermochemical cycle chosen for coupling to the fusion driver. The following ground rules were adopted in the selection of a specific thermochemical cycle for this study.

Chemistry

- The cycle should have some basis in experimental fact.
- Thermodynamic data should be available.
- Kinetic data on the important reactions should exist.

Engineering

- Cycle energy requirement characteristics should match the thermal energy source.
- Cycle should avoid highly corrosive environments wherever possible.
- Heat exchange should be minimized.

With these considerations in mind, a hybrid bismuth sulfate thermochemical cycle under development at LASL was selected for study. (A hybrid cycle is one that operates partly on thermal energy and partly on work energy, i.e., a low-temperature electrolysis step is incorporated within the cycle.)

B. The LASL Bismuth Sulfate Cycle

The reference bismuth sulfate cycle has already been analyzed,[1] but a review of its chemistry would help in understanding the present version of the cycle. The reference cycle has the following steps.

$$2H_2O(\ell) + SO_2(g) = H_2SO_4(aq) + H_2(g) \qquad \text{Elec. } 350\text{ K} \quad (1)$$

$$H_2SO_4(aq) + (1/3)Bi_2O_3(s) = (1/3)Bi_2O_3\cdot 3SO_3(s) + H_2O(\ell) \qquad 350\text{ K} \quad (2)$$

$$(1/3)Bi_2O_3\cdot 3SO_3(s) = (1/3)Bi_2O_3(\ell) + SO_3(g) \qquad 900\text{-}1200\text{ K} \quad (3)$$

$$SO_3(g) = SO_2(g) + (1/2)O_2(g) \qquad 1100\text{-}1500\text{ K} \quad (4)$$

Originally this cycle was devised as an alternative to those cycles employing H_2SO_4 as one of the reactants. In those cycles, the concentration of H_2SO_4 in solution is ~50 wt%. Those solutions are concentrated by evaporation to the azeotropic concentration at ~98 wt% acid before H_2SO_4 decomposition to water, sulfur dioxide, and oxygen. The highly corrosive nature of boiling H_2SO_4 solutions causes serious materials problems in the evaporation process. In addition, large heat penalties are possible unless one invokes multiple-effect evaporation, which involves expensive capital equipment.

Among the cycles employing H_2SO_4 processing are the hybrid sulfur cycle being developed by Westinghouse,[2] the General Atomic sulfur-iodine cycle,[3] and the Mark-13 sulfuric acid-bromine cycle being studied at the Euratom Center, Ispra, Italy.[4] At the respective locations, these three cycles are being studied in bench-scale apparatus capable of continuous operation to produce 100 ℓ of hydrogen per hour, and much attention is being devoted to the aforementioned materials problem.

At LASL, we sought to avoid hot concentrated H_2SO_4 corrosion and drying problems by precipitating an insoluble, anhydrous metal sulfate from the H_2SO_4 solutions, as shown in step (2)

above. The bismuth system was selected because insoluble anhydrous bismuth sulfate forms upon precipitation. If hydrated sulfate species, such as copper sulfate, were formed, additional heat would be required in the cycle. In step (2) of our reference cycle, the normal bismuth sulfate is formed by adding bismuth oxide to H_2SO_4 having a concentration greater than or equal to 52.7 wt%.[5] After drying, this sulfate can be decomposed thermally to bismuth oxide and sulfur trioxide, as shown in step (3). Sulfur trioxide further decomposes to sulfur dioxide and oxygen, which are separated to provide recycle sulfur dioxide for step (1), the electrochemical oxidation of sulfur dioxide to H_2SO_4 and hydrogen product. The electrochemical oxidation of sulfur dioxide to give hydrogen is the hybrid step. This reaction was first investigated by Bowman and Onstott at LASL,[6] and is a key step in the Westinghouse cycle.[2] In contrast to the other cycles, the LASL bismuth sulfate cycle involves solid-materials handling. Traditionally, liquids and gases are preferable to solids because of the problems of handling solids. The trade-off must be made between solids-handling and the difficulties (and expense) of handling highly corrosive, boiling H_2SO_4 streams. We plan future research in that direction.

C. Cycle Variations

Variations in the reference bismuth sulfate cycle are possible because of the intermediate bismuth oxysulfate compounds that result when normal bismuth sulfate, $Bi_2O_3 \cdot 3SO_3$, decomposes to bismuth oxide, Bi_2O_3, as illustrated in Fig. 1. In the reference design, we considered the removal of 1 mol of SO_3 from 1/3 mol of the normal bismuth sulfate to yield 1/3 mol of bismuth oxide [step (3)]. The endothermic heat requirement, 251 kJ/mol SO_3, was taken from tabulated thermodynamic data.[7] At the decomposition temperatures chosen, the bismuth oxide formed is in the liquid state, thus complicating the design of the decomposition reactors.[8] Recuperation of normal bismuth sulfate also requires a reasonably high acid concentration (52.7 wt% or higher), which in turn indicates an electrolyzer voltage of 0.6 V or higher. Our preliminary assessment of the reference cycle's efficiency was 41%.

To improve cycle efficiency, we devised alternatives that were based on the effect of cycling between two of the intermediate bismuth oxysulfate compounds in the decomposition sequence (see Fig. 1). An improved cycle would operate between the

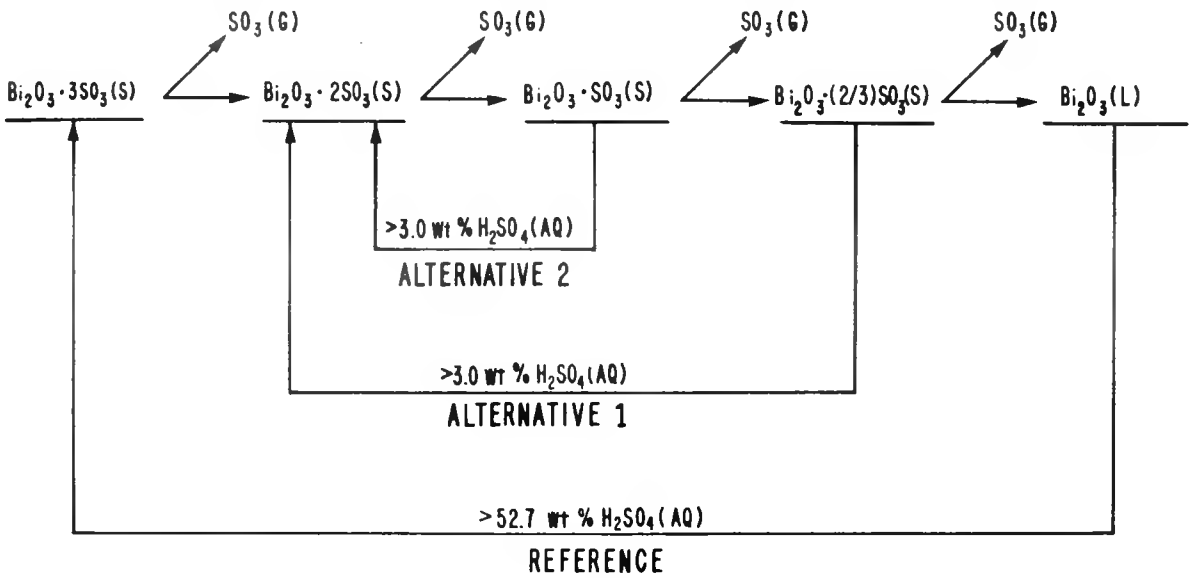

Fig. 1.
Bismuth sulfate decomposition alternatives.

compounds $Bi_2O_3 \cdot 2SO_3$ and $Bi_2O_3 \cdot SO_3$ (alternative 2 in Fig. 1). Experimental data on the endothermic heat of decomposition of $Bi_2O_3 \cdot 2SO_3$ to $Bi_2O_3 \cdot SO_3$ are included in Table I. Steps (2) and (3) presented for the reference cycle would be replaced by the following two steps:

$$Bi_2O_3 \cdot SO_3(s) + H_2SO_4(aq) = Bi_2O_3 \cdot 2SO_3(s) + H_2O(\ell) \qquad 350\ K \quad (5)$$

$$Bi_2O_3 \cdot 2SO_3(s) = Bi_2O_3 \cdot SO_3(s) + SO_3(g) \qquad 1000\text{-}1250\ K \quad (6)$$

The improved cycle, shown schematically in Fig. 2, has several advantages.

- The average endothermic heat requirement for the solid decomposition step would decrease from 251 to 172 kJ per mol of SO_3 removed.
- $Bi_2O_3 \cdot 2SO_3$ is the stable solid phase in contact with H_2SO_4 over a 3-52.7 wt% range.[5] In principle, the electrochemical oxidation of SO_2, step (1), could be carried out at a voltage lower than 0.6 V because of a reduction in the theoretical voltage as well as a possible reduction in overvoltage. Operation in the 10-20 wt% H_2SO_4 range would be feasible.
- Sulfuric acid is not handled at high concentrations or temperatures.
- Both sulfates present in step (6) would remain in the solid phase throughout the reaction and molten oxide would be avoided.
- Maximum temperatures required for solids decomposition can be lower than in other cycles.

The only foreseeable disadvantages of the improved cycle are the circulation of a larger amount of solid (1 mol of bismuth oxysulfate per mol of SO_3 removed, with attendant increased liquid entrainment) and a higher circulation rate for the H_2SO_4 electrolyte in the SO_2 electrolyzer. Another alternative would involve decomposition of $Bi_2O_3 \cdot 2SO_3$ to a stage represented by $Bi_2O_3 \cdot (2/3)SO_3$.

In practice, solid material corresponding to $Bi_2O_3 \cdot SO_3$ or $Bi_2O_3 \cdot (2/3)SO_3$ would be removed from the decomposition reactor for contact with 10-20 wt% acid from the electrolyzers to produce $Bi_2O_3 \cdot 2SO_3$ starting material. For simplicity, we considered removing only 1 mol of SO_3 as far as $Bi_2O_3 \cdot SO_3$ in the optimized design. Again, in an actual process, the starting material would be slightly more enriched in SO_3 than suggested by $Bi_2O_3 \cdot 2SO_3$ as a result of reaction between the occluded H_2SO_4 and the $Bi_2O_3 \cdot 2SO_3$ precipitate.

We are searching for continuous methods of decomposing $Bi_2O_3 \cdot 2SO_3$. Solid-handling approaches include fluidized beds, rotary kilns, and vertical moving beds. In early testing of the

TABLE I

BISMUTH SULFATE DECOMPOSITION DATA

Reaction	T(K)	ΔH (kJ/mol SO_3)	Wt% H_2SO_4 in Equilibrium with Sulfate[a]
$Bi_2O_3 \cdot 3SO_3 = Bi_2O_3 \cdot 2SO_3 + SO_3$	875	161	>52.7
$Bi_2O_3 \cdot 2SO_3 = Bi_2O_3 \cdot SO_3 + SO_3$	1120	172	~3-10
$Bi_2O_3 \cdot SO_3 = Bi_2O_3 \cdot (2/3)SO_3 + (1/3)SO_3$	>1200	---	<3.0
$Bi_2O_3 \cdot (2/3)SO_3 = Bi_2O_3 + (2/3)SO_3$	>1250	---	---
Overall			
$Bi_2O_3 \cdot 3SO_3 = Bi_2O_3 + 3SO_3$	875	251 (7)	>52.7

[a]Data from Ref. 5.

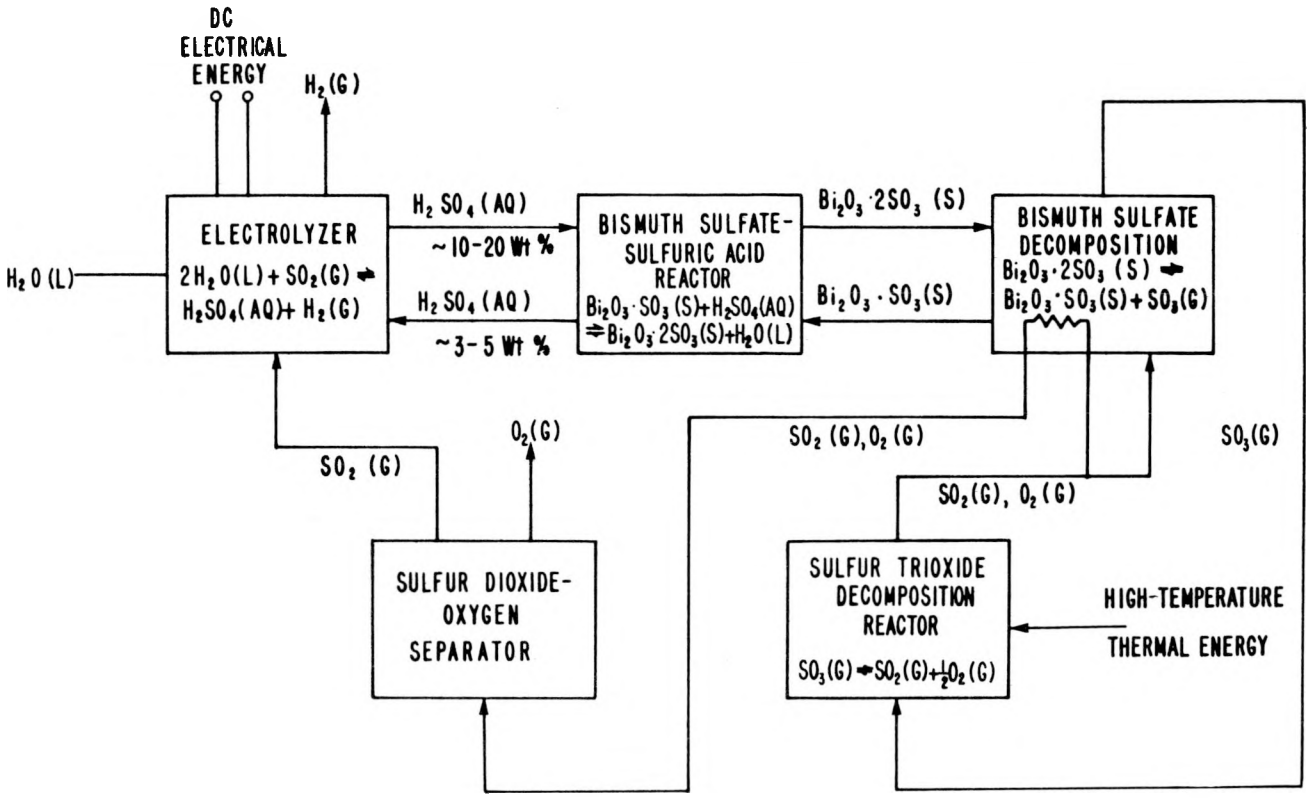

Fig. 2.
Schematic of the LASL bismuth sulfate hybrid cycle.

fluidized-bed alternative, we found a major variable to be the physical aspect of the solid sulfate material, for example, the particle size and shape, the particle size distribution, and the tendency to agglomerate or pill.

II. EXPERIMENTAL VERIFICATION OF CYCLE

The experimental bases for the foregoing observations are shown in Figs. 3 and 4. Thermodynamic data on the endothermic heat of reaction for

$$Bi_2O_3 \cdot 3SO_3(s) = Bi_2O_3 \cdot 2SO_3(s) + SO_3(g) \quad (7)$$

and

$$Bi_2O_3 \cdot 2SO_3(s) = Bi_2O_3 \cdot SO_3(s) + SO_3(g) \quad (8)$$

were obtained from isothermal batch experiments. The SO_3 pressure obtained from total $(SO_3/SO_2/O_2)$ pressure measurements over samples of bismuth oxysulfate of known composition is shown as a function of temperature in Fig. 3. Straight-line plots of log P_{SO_3} vs 1/T give a value of 161 kJ/mol (38.4 kcal/mol) for the $Bi_2O_3 \cdot 3SO_3$ decomposition and 172 kJ/mol (41.2 kcal/mol) for the $Bi_2O_3 \cdot 2SO_3$ decomposition.

Kinetic data for the decomposition of $Bi_2O_3 \cdot 3SO_3$ starting material are shown in Fig. 4. The data show the rate of SO_3 removal as a function of time at temperatures of 1050, 1150, and 1240 K. In all cases, after 30 min or more the normal bismuth sulfate decomposed to yield a solid material having the approximate stoichiometric formula of $Bi_2O_3 \cdot (2/3)SO_3$ and releasing 2.33 mols of SO_3. The decomposition time for the release of 2 mols of SO_3 (to form $Bi_2O_3 \cdot SO_3$) is dependent on the run temperature. At 1240 K, ~1.5 min are required for the decomposition of $Bi_2O_3 \cdot 3SO_3$ to $Bi_2O_3 \cdot SO_3$. Less time (roughly half) would be required for the intermediate step, $Bi_2O_3 \cdot 2SO_3$ to $Bi_2O_3 \cdot SO_3$. In these experiments the reaction rate probably is determined by

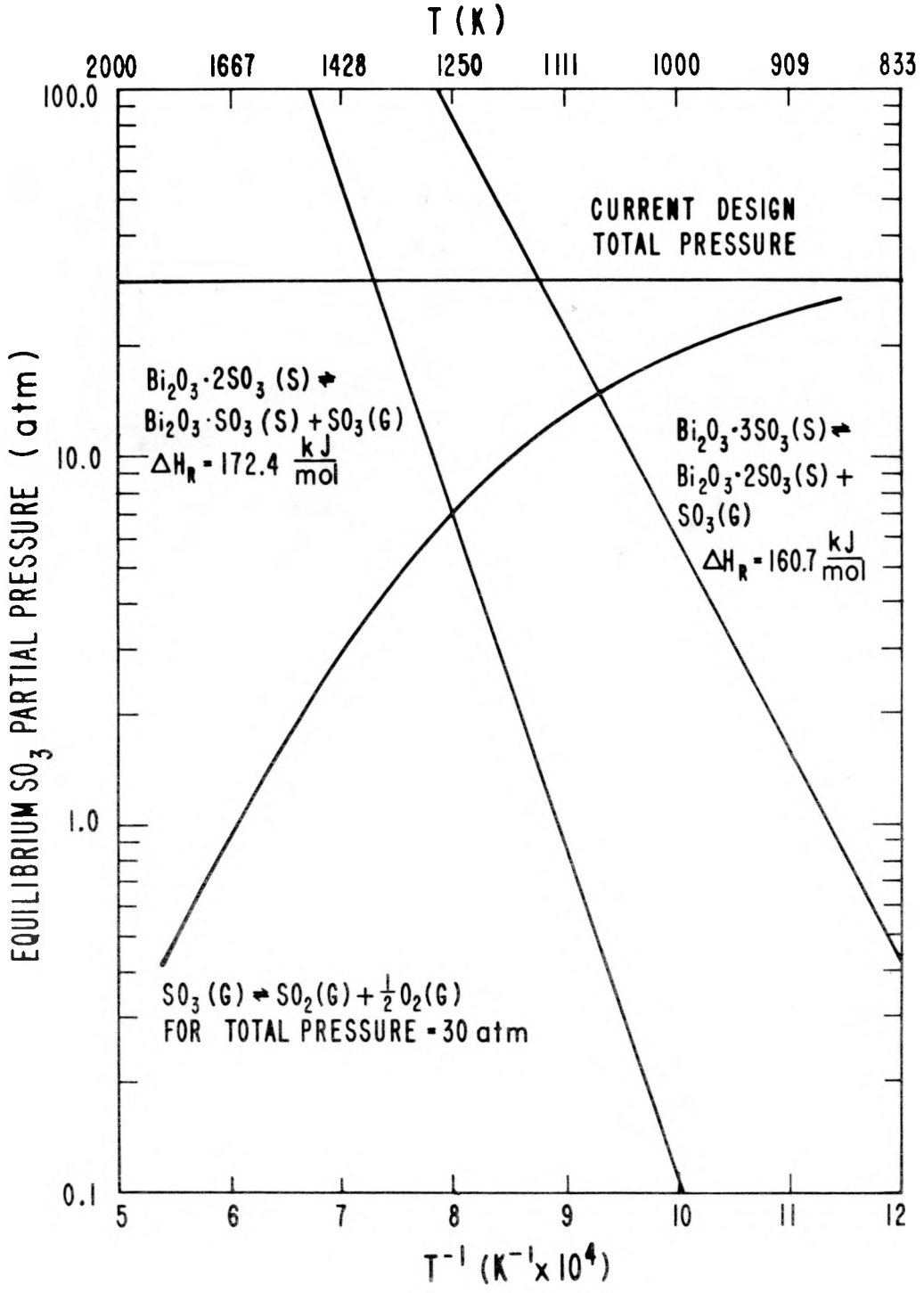

Fig. 3.
Equilibrium data for bismuth sulfate and bismuth oxysulfate decomposition.

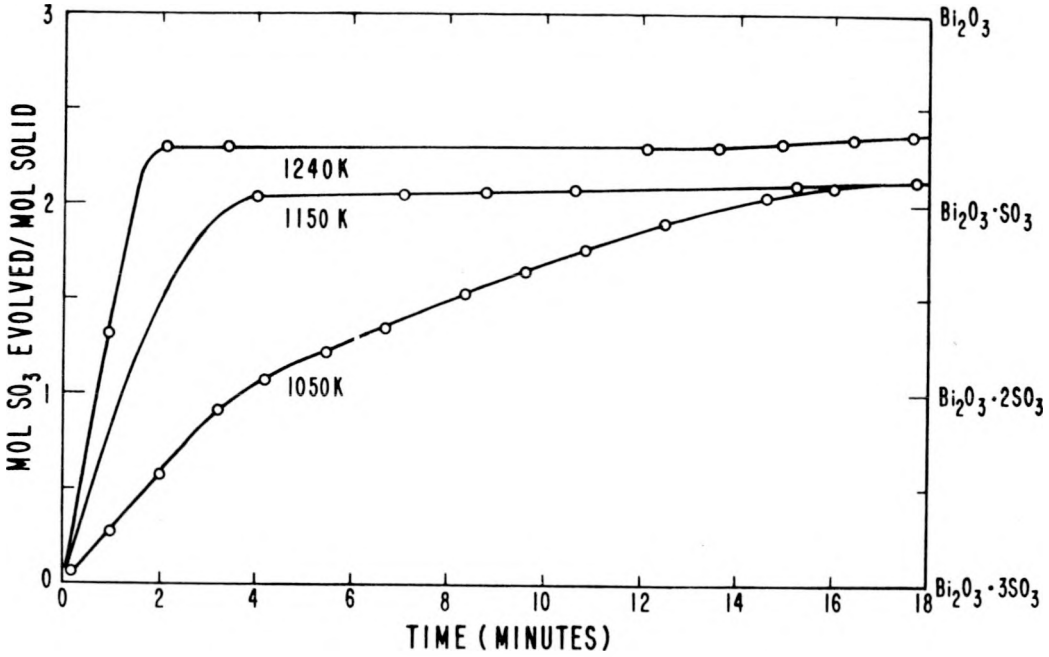

Fig. 4.
Kinetics of bismuth sulfate decomposition.

temperature-dependent kinetics rather than by heat transfer. In large industrial reactors, heat transfer may play a larger role, depending on particle size, etc. In fluidized beds, heat and mass transfer rates are large; therefore, reaction times would be temperature-dependent.

Further details on the thermodynamic and kinetic experiments are given later in this report.

III. PROCESS DESIGN OF CYCLE

A thermochemical process design has been developed for both the reference and the improved versions of the LASL bismuth sulfate cycle. The design aims were to produce an engineering flow sheet, compute mass and energy balances, and obtain a value for the thermal efficiency of the cycle. The eventual aim is to obtain the cost of hydrogen production for such a process. For ease of analysis the cycle was split into low-temperature and high-temperature operations. The flow sheet for the low-temperature portion is shown in Fig. 5; that for the high-temperature portion is in Fig. 6.

A fusion reactor deposits neutrons in a high-temperature boiling lithium blanket at 1500 K. Thermal energy from the isothermal "lithium boiler" is transferred directly to a $SO_3/SO_2/O_2$ process stream for the high-temperature portion of the cycle. One heat exchanger thus provides all the primary thermal energy for the cycle. Heat from a low-temperature (800 K) portion of the fusion blanket provides the electric power generation energy for the electrolysis section located in the low-temperature portion of the cycle. We assumed equilibrium compositions in all gas streams containing $SO_3/SO_2/O_2$, except after rapid quenching to temperatures below 800 K. Data for this equilibrium were obtained from thermodynamic compilations.[9] For pipeline transmission, hydrogen must be at pressures substantially above atmospheric pressure. We chose a design pressure of 3 MPa (30 atm) as the operating pressure in the electrolyzer vessel to yield a hydrogen product at this pressure for outside delivery and chose the same pressure in the decomposition reactors to minimize their size. In this design, we also assumed negligible thermal and pumping (transfer) losses in comparison with the thermal energy flows. Thus the high-temperature decomposers are designed to operate isobarically, neglecting temporarily the pressure drops through the reactors. Inclusion of these factors would necessitate minor downward adjustments to the calculated estimate of the cycle's efficiency.

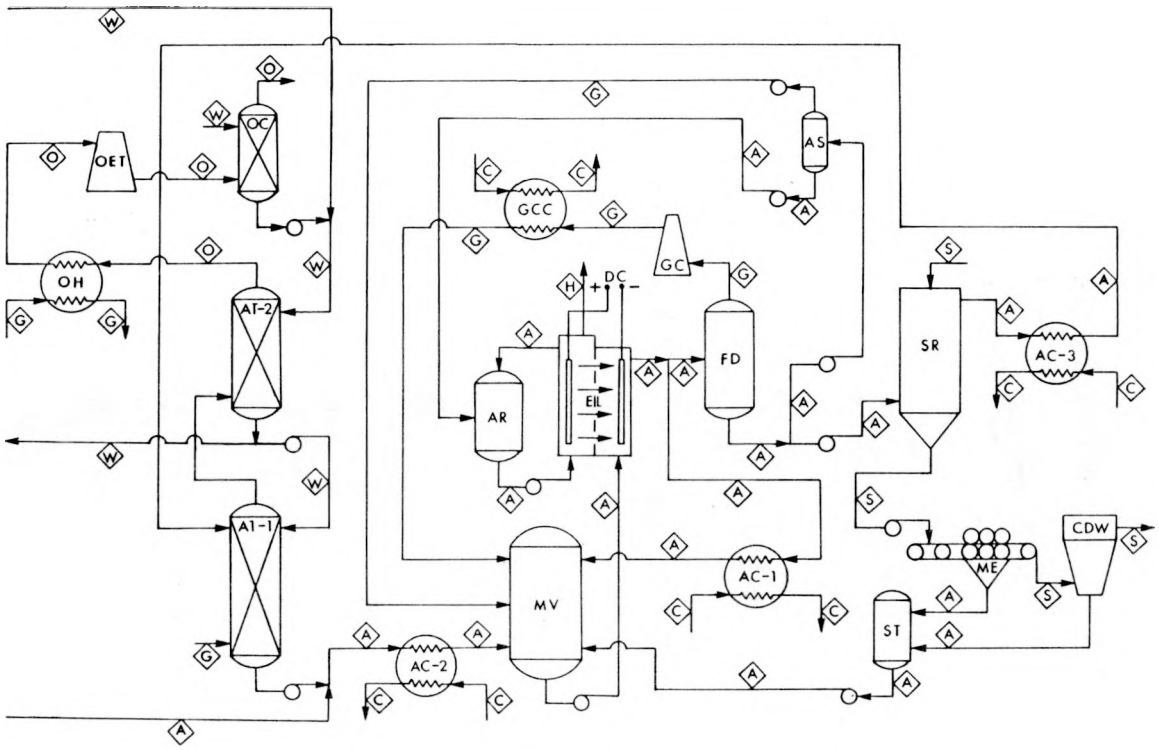

Fig. 5.

Flowsheet for low-temperature portion of the LASL bismuth sulfate cycle. A, aqueous H_2SO_4 with and without SO_2; AC-1, -2, -3, acid coolers; AR, acid reservoir; AS, acid separator; AT-1, -2, SO_2 absorption towers; C, cooling water; CDW, dewatering centrifuge; EL, electrolyzer; FD, flash drum; G, SO_2-containing gas; GC, gas compressor; GCC, gas cooler-condenser; ME, mechanical expression rollers; MV, mixing vessel; O, predominantly oxygen gas; OC, oxygen cleanup tower; OET, oxygen expansion turbine; S, solids; SR, solids reactor; ST, surge tank; W, predominantly water.

IV. LOW-TEMPERATURE PORTION OF CYCLE

Three major components of the process are included in the low-temperature portion: the SO_2 oxidation electrolyzers, the bismuth oxysulfate precipitation reactors, and the units for separating SO_2 from O_2 and the extraction of energy from the oxygen stream by expansion to ambient conditions. This portion of the cycle is illustrated in Fig. 5. In the electrolytic step, (6), sulfurous acid is oxidized and hydrogen forms simultaneously at the cathode. Migration of sulfurous acid to and subsequent formation of sulfur at the cathode must be avoided. This problem was first overcome by providing a slight catholyte overpressure in conjunction with a suitable porous membrane. In our design, we assumed use of a semipermeable, ion-conducting membrane that reduces sulfurous acid migration into the cathode compartment of the electrolytic cell. The electrolytic cell design parameters are: cell voltage, 0.45 V; current density, 2000 A/m^2; temperature, 350 K; pressure, 3MPa (30 atm); and acid concentration, 10-20 wt%. Experiments are under way to verify the choice of these operating parameters for the electrolysis portion of the cycle.

The effluent acid stream at 20 wt% is cooled by heat exchange before being reacted with the bismuth oxysulfate ($Bi_2O_3 \cdot SO_3$) effluent from the decomposer vessels. The reactors produce a wet $Bi_2O_3 \cdot 2SO_3$ precipitate that is returned to the high-temperature portion of the cycle. The reaction of $Bi_2O_3 \cdot SO_3$ with H_2SO_4 liberates heat estimated at 38 kJ/mol—roughly half the heat release for the reaction of bismuth oxide with H_2SO_4 to form $Bi_2O_3 \cdot 2SO_3$. This heat raises the temperature of the

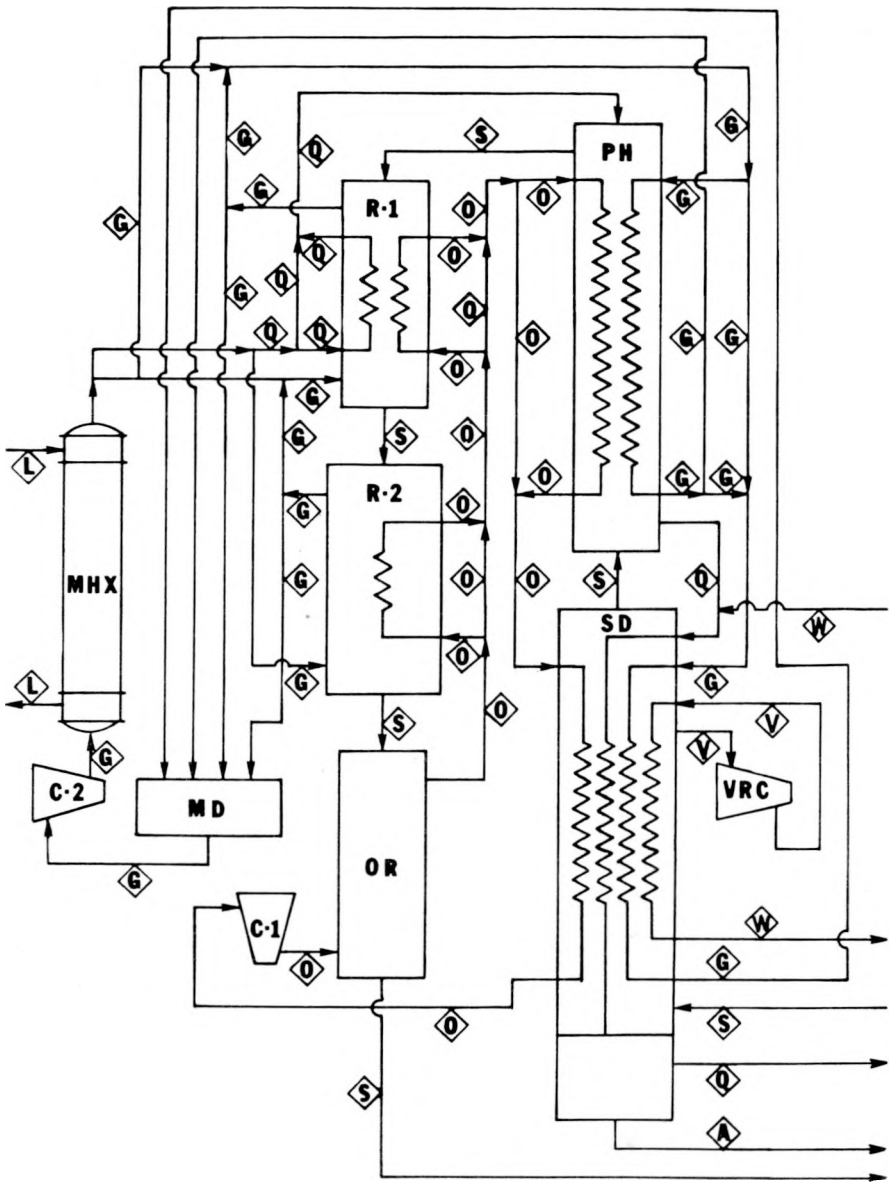

Fig. 6.

Flow sheet of the high-temperature portion of the LASL bismuth sulfate cycle. A, aqueous H_2SO_4 stream; C-1, -2, compressors; G, $SO_3/SO_2/O_2$ gas stream; L, lithium stream; MD, mixing drum; MHX, main heat exchanger; O, oxygen heat recuperation stream; OR, direct contact oxygen heat recuperator; PH, solids preheater; Q, $SO_3/SO_2/O_2$ gas quench stream; R-1, -2, solids decomposition reactors; S, bismuth oxysulfate solids stream (including occluded aqueous acid); SD, slurry drier; VRC, vapor recompressor.

acid effluent from the bismuth oxysulfate reactors. The acid effluent is then introduced into a series of gas absorbers where it separates SO_2 from the SO_2/O_2 stream leaving the decomposers. This operation recovers SO_2, which is then recycled with the acid back to the electrolyzers. The oxygen stream from the absorbers contains trace amounts of SO_2, which is further reduced by contact with the water that enters the cycle. After final scrubbing, the oxygen stream is heated, expanded to recover useful work, and vented to the atmosphere at close to ambient conditions.

Other proposed SO_2/O_2 separation schemes that depend on the cryogenic separation of SO_2 by its liquefaction from noncondensable oxygen (at the specified temperatures) may be flawed because of oxygen's considerable solubility in liquid SO_2.[10] The temperature coefficient of solubility for oxygen is positive, thus the liquid SO_2 must be at even lower temperature for better oxygen removal.

V. HIGH-TEMPERATURE PORTION OF CYCLE

The high-temperature portion of the cycle includes the bismuth sulfate drying step, the bismuth sulfate decomposition, and the SO_3 decomposition steps. Isothermal energy at 1500 K from condensing lithium vapor supplies heat to the high-temperature portion of the cycle by driving to the right the endothermic reaction $SO_3 = SO_2 + (1/2)O_2$. The shift of the equilibrium to the left when the gas mixture drops to lower temperature evolves heat that is used for the endothermic decomposition of entering $Bi_2O_3 \cdot 2SO_3$ in a chemical heat-pipe mechanism. In this manner, primary heat from the fusion reactor is coupled to the high-temperature portion of the cycle in a single heat exchanger. The other heat exchangers shown on the flow sheet (Fig. 6) are for internal heat recovery, i.e., preheating incoming "cold" streams with exiting "hot" streams.

Equilibrium pressures for the $SO_3/SO_2/O_2$ system are well known[9] and data for this system, in the form of P_{SO_3} are plotted in Fig. 3 as a function of temperature at a total pressure of 3 MPa (30 atm). The crossover point with the $Bi_2O_3 \cdot 2SO_3$ decomposition line occurs at 1250 K. Above that temperature SO_3 obtained from the decomposing bismuth oxysulfate will equilibrate with SO_2 and O_2. The corresponding temperature for the $Bi_2O_3 \cdot 3SO_3$ decomposition is 1010 K.

With reference to the flow sheet in Fig. 6, incoming $Bi_2O_3 \cdot 2SO_3$, mechanically dewatered to 87 wt% solids and containing roughly 5 mols of water per mol of entering solid is dried by indirect contact with warm streams of quenched $SO_2/O_2/SO_3$ and steam. By recompression of the steam (produced from the water contained in the solids) most of the heat supplied during evaporation can be recovered. An internal recycle stream of oxygen provides additional heat. Exiting at the bottom of the drier are a gas stream composed mainly of SO_2 and O_2 and a liquid stream containing water and H_2SO_4. The dry solids exit at the top of the drier vessel, where they contact directly a quenched $SO_2/O_2/SO_3$ stream that comes directly from the SO_3 decomposer (primary heat exchanger) and that is essentially unchanged in composition from its equilibrium at 1500 K and 3 MPa (30 atm). Heat exchange between these streams raises the temperature of the dried $Bi_2O_3 \cdot 2SO_3$. Additional heat to raise the temperature of the solids is obtained from a recycle $SO_2/O_2/SO_3$ stream as well as from the recycle oxygen.

The dried and heated $Bi_2O_3 \cdot 2SO_3$ solids are now introduced into a series of decomposition reactors (R-1 and R-2 in Fig. 6), where they come into direct contact with a $SO_2/O_2/SO_3$ gas mixture from the primary heat exchanger. For the gas phase we assumed equilibrium conditions at the inlet and outlet temperatures of these decomposer vessels. In the decomposers the solids are heated by sensible heat exchange with the hotter gases and by the heat of reaction given up as some of the SO_2 and O_2 shifts toward SO_3. This forms the heat recovery portion of the chemical heat-pipe mechanism mentioned earlier. The process drastically reduces the gas flows from what they would have to be if only sensible heat were exchanged. The decomposition reactors, which serve as contacting devices between solids and gases, could have configurations such as fluidized beds, moving beds, or rotary kilns. Decomposer reactor design would involve considerations of temperature, pressure, reaction rate, and heat transfer. Also, the solids themselves may act as catalytic surfaces for the $SO_2/O_2/SO_3$ equilibrium. If the solid material proves to be catalytically inactive, catalyst coatings might have to be provided on interior surfaces of the decomposer vessels.

We considered the removal of 1 mol of SO_3 per mol of entering $Bi_2O_3 \cdot 2SO_3$ as well as the removal of 1.33 mols of SO_3 to yield a product of $Bi_2O_3 \cdot 2SO_3$ or $Bi_2O_3 \cdot (2/3)SO_3$, respectively. Before its discharge, the solid material is cooled by the internally recycling oxygen stream. Then it is returned to the low-temperature portion of the cycle for subsequent contact with H_2SO_4 and regeneration to the $Bi_2O_3 \cdot 2SO_3$ starting material.

VI. ENERGY BALANCE AND EFFICIENCY OF CYCLE

To obtain quantitative data for the performance of this cycle relative to other cycles and to water electrolysis, we made parametric analyses of the cycle's energy balance over a wide range of operating conditions.

An enthalpy balance model (Fig. 7) was constructed to obtain Q_H, the endothermic heat per mol of H_2 required in the high-temperature portion. We assumed negligible heat losses and a 25 K temperature difference for heat transfer. The endothermic heat requirement can be expressed as:

$$Q_H = \sum_{\text{in}} n_i h_i(350\ \text{K}) - \sum_{\text{out}} n_j h_j\ (375\ \text{K}) \qquad (9)$$

where n_i = mols component i, and h_i = molar enthalpy of components. The variables include maximum stream temperature, 1275-1675 K; system pressure, 2 MPa (20 atm)-5 MPa (50 atm); mols SO_3 removed, 1.0 and 1.33; mols H_2O entering with $Bi_2O_3 \cdot 2SO_3$, 0-20 (as 15 wt% H_2SO_4).

Figure 8 shows the results of an evaluation in which the variation of Q_H is plotted against the number of entering mols of water as a function of maximum temperature and the number of mols of SO_3 removed. The minima in the curves result from two effects: (a) the 25 K difference between the feed and outlet streams and (b) the recombination of unreacted SO_3 with water in the outlet stream to form H_2SO_4 and the resulting release of ~289 kJ/mol. Less endothermic heat is required to transform $Bi_2O_3 \cdot 2SO_3$ to $Bi_2O_3 \cdot SO_3$ than to $Bi_2O_3 \cdot (2/3)SO_3$; however, this must be balanced against a small increase in materials circulation.

For a representative energy balance and efficiency calculation, we chose the following process conditions: maximum temperature, 1475 K; pressure, 30 atm; mols SO_2 removed, 1.0; mols H_2O entering, 5.0. The overall energy balance for the cycle is given in Table II and is shown schematically in Fig. 9 for these conditions. An overall cycle efficiency of 50.8% is predicted. Details of the balance are given below.

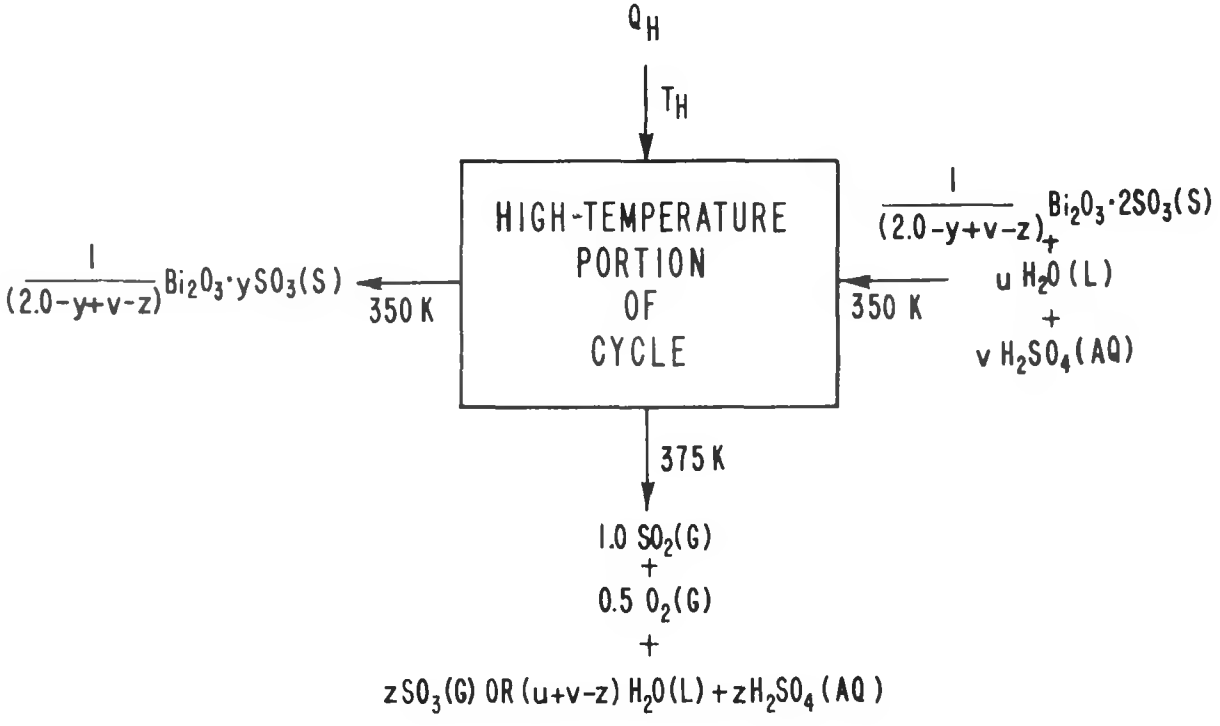

Fig. 7.
Energy balance model for the high-temperature portion of the cycle.

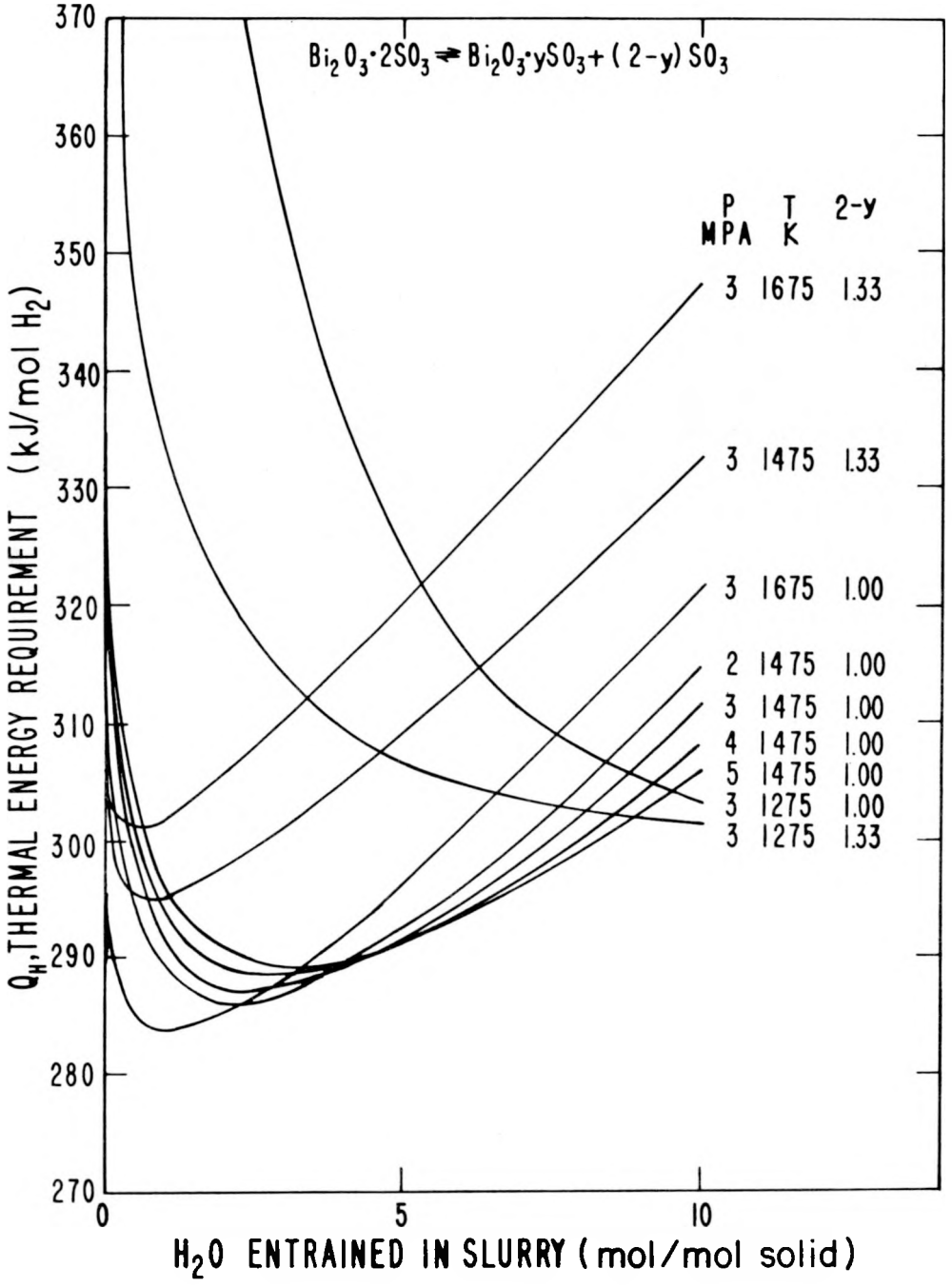

Fig. 8.
Parametric analysis of the thermal energy requirement for the high-temperature portion of the cycle.

A. High-Temperature Portion of the Cycle

High-temperature fusion energy in the form of heat from a lithium boiler operating at 1500 K provides the input to the high-temperature portion of the cycle, which consists of three batteries: Battery A—Solids dewatering, Battery B—Solids decomposition, and Battery C—SO_3 decomposition.

A thermal energy balance was performed for each battery to identify the input and output of energy,

TABLE II

CYCLE ENERGY BALANCE
(In kJ/mol H_2)

	Heat Required	Heat Available	Heat Rejected	Work[a] Required	Work[a] Available
HIGH-TEMPERATURE PORTION					
Battery A—Solids Dewatering					
Slurry heating, water evaporation, acid reaction with $Bi_2O_3 \cdot 2SO_3$	337				
Vapor recompression				23	
Condensation, cooling		248			
Cooling of $SO_2/O_2/SO_3$		16			
SO_3 reaction to form H_2SO_4		66			
Net		7			23
Battery B—Solids Decomposition					
Solids heating	171				
Solids decomposition	196				
Solids cooling		170			
Net		197			
Battery C—SO_3 Decomposition					
SO_3 heating	16				
SO_3 decomposition	99				
$So_2/O_2/SO_3$ cooling		70			
Gas compression (circulation)				25	
Net		45			25
LOW-TEMPERATURE PORTION					
Battery D—SO_2/O_2 Separation					
Acid heating	25				
Oxygen heating	20				
Turbine expansion					42
SO_2 compression			55	35	
Net		45			7[b]
Battery E—Electrolyzer					
Electrolyzer			54	228	
Net					228
Battery F—Solids/Acid Reactor					
Reactor			38		
Totals (net)		294			269

[a]Heat-to-work conversion = 0.38.

[b]Available.

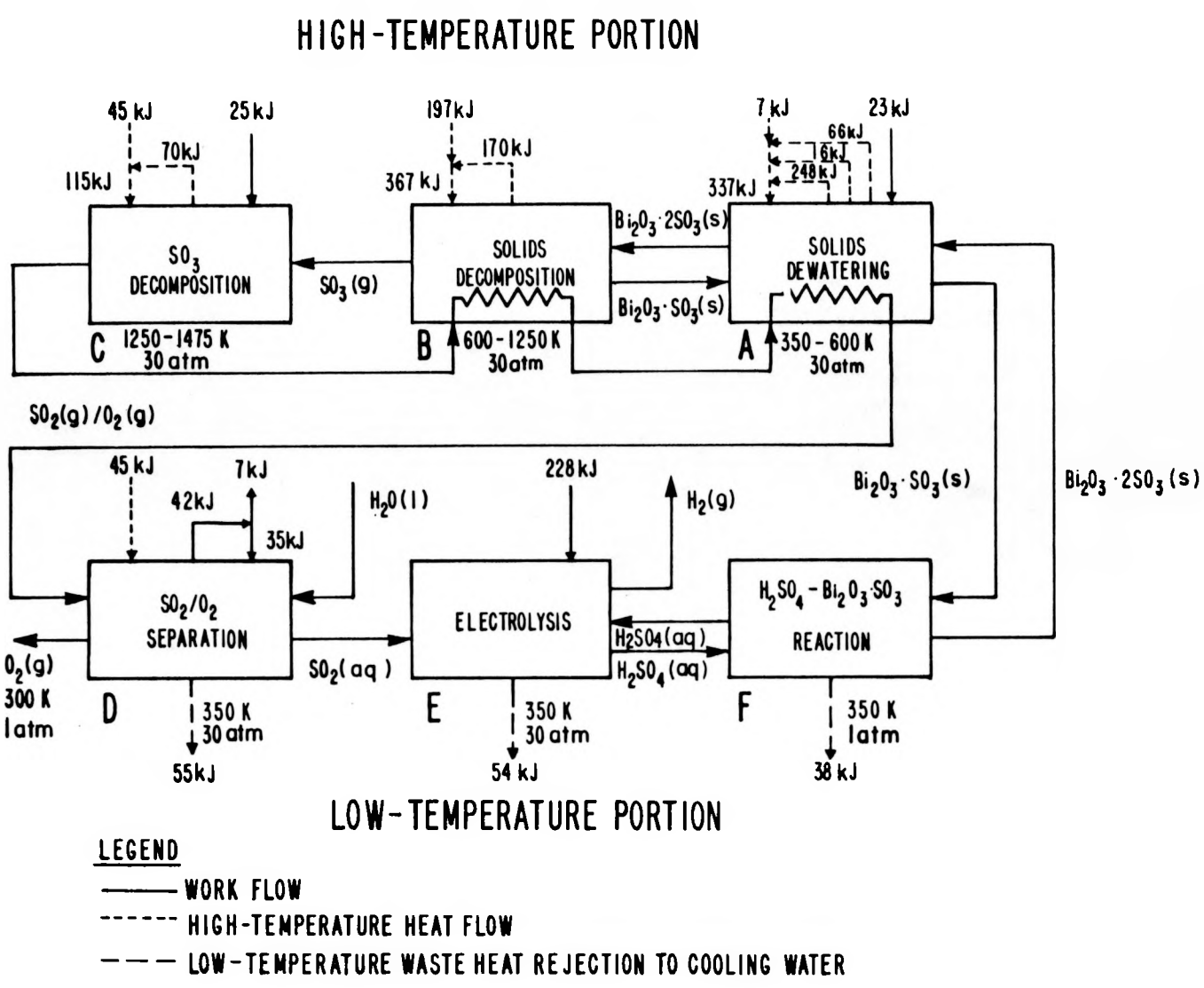

Fig. 9.
Cycle energy balance.

including work. One mol of hydrogen production (1 mol of water decomposed) was used as the basis of calculation and work is expressed as its thermal equivalent, assuming a 38% conversion from heat to work.

1. Battery A—Solids Dewatering. The function of Battery A is to dry the incoming $Bi_2O_3 \cdot 2SO_3$ solids and to perform that task by recovering as much heat as possible from hot streams and exothermic reactions. Entering this battery is $Bi_2O_3 \cdot 2SO_3$ containing 5 mols of water per mol of solid at 350 K and 30 atm. The water enters in the form of 15 wt% H_2SO_4 and the acid is assumed to react with the solid to form some $Bi_2O_3 \cdot 3SO_3$. These two solids and any unattached water leave the battery at 600 K and 30 atm. The heat duty for this operation is 337 kJ.

To permit use of the latent heat of water vaporization for heat recovery, a vapor recompression to 40 atm pressure is performed on the steam, which amounts to a work input of 23 kJ. As much as 248 kJ can be recovered from the steam by this operation. Other heat recovery operations performed in this battery include the cooling of a gas quench stream

(16 kJ) and the reaction of undecomposed SO_3 with the condensate to form H_2SO_4 (66 kJ). Net energy requirements for Battery A are 7 kJ (thermal) and 23 kJ (work)—a total of 30 kJ.

2. Battery B—Solids Decomposition. Battery B uses a large amount of heat for decomposing the entering solids to $Bi_2O_3 \cdot SO_3$ and SO_3. Heat requirements are 171 kJ for heating the solids from 600 to 1250 K and 196 kJ for decomposing them. Cooling of the decomposed solids from 1250 to 350 K permits recovery of 170 kJ. Thus the heat demand for Battery B is 197 kJ, which is supplied by a chemical heat-pipe scheme involving the production of SO_3 from SO_2 and O_2 and avoiding heat transfer through a solid wall.

3. Battery C—SO_3 Decomposition. Battery C operates at the highest temperature of the cycle (1475 K). A 25 K difference was arbitrarily chosen for heat transfer. Heat loads are 16 kJ for heating SO_3 from 1250 to 1475 K and 99 kJ for the decomposition of SO_3. Heat recovered from cooling the SO_2 and O_2 products and unconverted SO_3 reactant amounts to 70 kJ. The net thermal demand for Battery C is 45 kJ. Included is a work input of 25 kJ for gas circulation through the reactors.

B. Low-Temperature Portion of Cycle

The low-temperature portion of the cycle operates at 350 K and consists of three batteries: Battery D—SO_2/O_2 separation, Battery E—Electrolyzer, and Battery F—Solids/acid reactor.

1. Battery D—SO_2/O_2 Separation. The first function of Battery D is to rid the electrolyzer effluent of most of its SO_2 by a flash operation, thereby permitting later use of the H_2SO_4 at atmospheric pressure. The flashed SO_2 is compressed for recycle to the electrolyzer—a work input of 35 kJ. The remaining SO_2 is driven off by a heated sidestream of acid so that the catholyte will be SO_2-free and sulfur will not form in the electrolyzer. An estimated 25 kJ of heat are required for that step. Reject heat (at 350 K) of 55 kJ results from absorption of SO_2 from the SO_2/O_2 gas mixture. Heating the purified oxygen stream to 1475 K for generating work in a turbine expander requires 20 kJ of heat. Battery D thus requires 45 kJ of heat and gives an estimated 7-kJ work gain.

2. Battery E—Electrolyzer. We assume a working voltage of 0.45 V, at an acid concentration of 15 wt% and a current density of 2000 A/m^2. The electrolyzer is designed for operation at 350 K and 30 atm. On the basis of these conditions, we calculate a 228-kJ work input to the electrolyzer. Heat rejected from the electrolyzer because of losses amounts to 54 kJ.

3. Battery F—Solids/Acid Reactor. $Bi_2O_3 \cdot SO_3$ reacting with H_2SO_4 releases 38 kJ at 350 K to cooling water.

C. Overall Efficiency of Cycle

The cycle's efficiency is computed from the values given in Table II. The net heat requirement is 294 kJ and the work requirement is 269 kJ—a total of 563 kJ. The efficiency is $\eta = 286/563 = 0.508$ (50.8%).

Another parametric analysis was made to evaluate the effect of three major system variables on the cycle's efficiency. The variables chosen for this analysis were the electrolyzer cell voltage, the endothermic heat requirement in the high-temperature portion, and the maximum stream temperature in the cycle. Held constant were the system pressure at 3 MPa, the mols of SO_3 removed at 1.0, and the mols of water entering the high-temperature portion at 5.0. The results of this analysis are shown in Fig. 10. In the case of the variation of cell voltage, the temperature was kept constant at 1475 K and the endothermic heat at 285 kJ/mol H_2. In the other two cases, the cell voltage was kept at 0.45 V (228 kJ/mol, heat equivalent).

Of the three variables investigated, the cycle's efficiency was most affected by the electrolyzer voltage and the endothermic heat requirement. The efficiency is extremely sensitive to variation in electrolyzer voltage. The effect of maximum stream temperature variation is important primarily because it varies the equilibrium yield in the $SO_3 = SO_2 + (1/2)O_2$ reaction, hence changes the composition of the gas mixture leaving the high-temperature portion of the cycle. It also affects the rate of solids circulation.

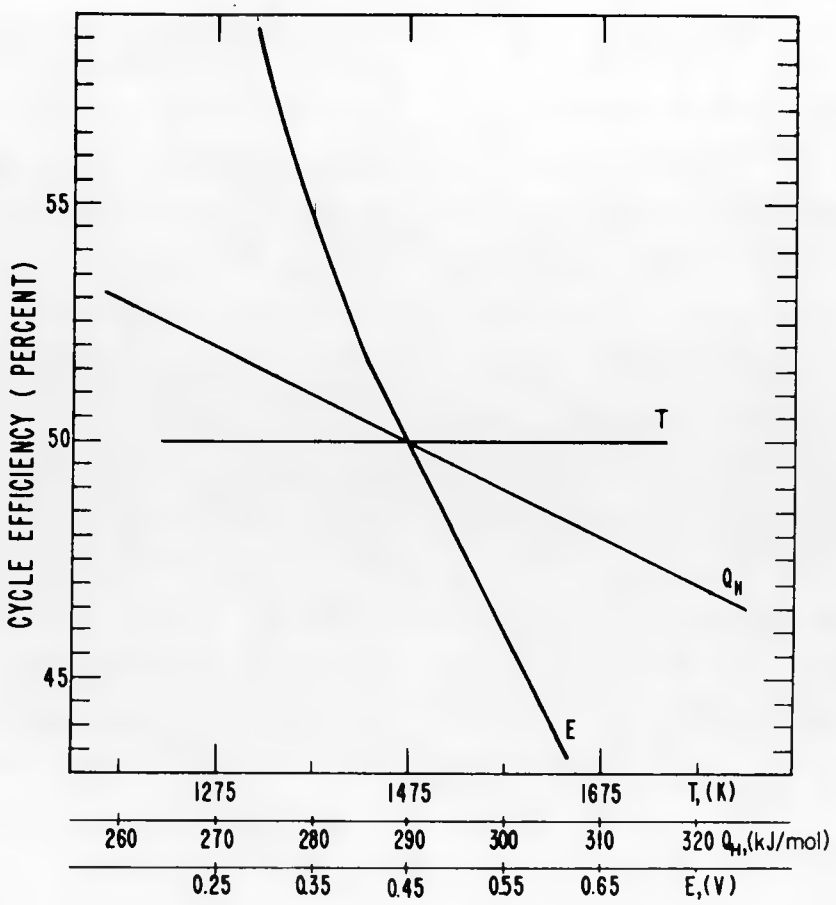

Fig. 10.
Parametric analysis of cycle efficiency.

The variation in overall system pressure indicated small changes in Q_H between 20-50 atm. Varying the system pressure in a gaseous system would necessitate changes in equipment sizes and structural requirements, thus influencing the capital costs of the cycle.

For high overall thermal efficiency, it is important to choose operating conditions that minimize thermal and electrical energy expenditure. In the bismuth sulfate cycle, these conditions are fulfilled by the choice of a reasonably high maximum stream temperature (1475 K), high system pressure (3 MPa), low electrolyzer voltage (0.45 V), 1 mol of SO_3 removed per mol of entering $Bi_2O_3 \cdot 2SO_3$, and < 5 mols of water entering the high-temperature portion of the cycle.

VII. MATERIALS

In the low-temperature portion of the cycle, plastic-lined steel is the favored material for components in contact with 350-400 K H_2SO_4. At temperatures from 400-800 K, an acid brick can be used to line the equipment. For the high-temperature portion of the cycle, where we have to contain bismuth oxysulfates as well as dry SO_3, SO_2, and O_2, the high-temperature form of SiO_2 or a recently announced oxidation-resistant SiC sponge,[11] which have capabilities to 1800 K, could be used. These materials problems require more detailed investigation.

VIII. CONCLUSIONS OF STUDY

The LASL bismuth sulfate cycle is a promising approach to producing hydrogen from a high-temperature process heat source (1500 K) such as that from a fusion or solar reactor. It avoids the problem of evaporating H_2SO_4 solutions and has an estimated 50% efficiency, based on a flow-sheet analysis. Crucial issues still to be resolved are the demonstration of low-voltage electrolysis under production conditions, the recovery of latent heat of vaporization from drying solid $Bi_2O_3 \cdot 2SO_3$, and the handling of large amounts of solids in a high-temperature decomposer vessel.

We have not yet evaluated the cycle on economic grounds. However, despite the solids-handling problem, potential higher efficiencies may lead to hydrogen costs lower than those for other cycles being developed.

IX. EXPERIMENTAL WORK ON THE BISMUTH SULFATE DECOMPOSITION

A. Kinetics

Work during this period was concentrated on the rate of decomposition of $Bi_2O_3 \cdot 3SO_3$ to SO_3 and an oxysulfate or Bi_2O_3. In most of the experiments the sample was brought to ~600 K at the top of the furnace and lowered in 0.2 min to the center of the furnace at the maintained temperature. The SO_3 was removed by a helium carrier gas and absorbed in water. Reaction progress was followed by titration with standardized sodium hydroxide. Results from the titrations and sample weight loss agreed within ~1%. In a typical run, the temperature (as measured by a chromel-alumel thermocouple) was within 2 deg of the furnace temperature in less than 2 min after the sample was introduced.

Figure 4 gives the experimental results for runs made at 1050, 1150, and 1240 K, and the evolution of SO_3 is shown as a function of time. At 1050 K, the following observations were made.

- The first SO_3 evolves in ~3 min.
- The second SO_3 evolves in ~5 min.
- During the evolution of the first SO_3, the SO_3 pressure reached 0.44 atm.

An additional 1/3 mol of SO_3, evolved over a ~2-h period, may correspond to the formation of $Bi_2O_3 \cdot (2/3)SO_3$, analogous to $Sb_2O_3 \cdot (2/3)SO_3$, which has a known crystal structure.

Two runs were made at 1150 K. The rate curve in Fig. 4 shows a sharp break upon evolution of 2 mols of SO_3. At 1240 K, an abrupt break occurs on evolution of 2.3 mols of SO_3 in about 1.5-min reaction time—the fastest rate we obtained. In that run the SO_3 pressure was 0.6 atm.

The pattern of the sharp breaks obtained after evolution of 1 or 2 mols of SO_3 suggests that the equilibria involve solids of integral stoichiometry and not solid solutions:

$$Bi_2O_3 \cdot 3SO_3 = Bi_2O_3 \cdot 2SO_3 + SO_3 \quad (7)$$

$$Bi_2O_3 \cdot 2SO_3 = Bi_2O_3 \cdot SO_3 + SO_3 \ . \quad (8)$$

Therefore, the d-spacing in the x-ray diffraction pattern of the product obtained when $Bi_2O_3 \cdot 3SO_3$ decomposes partially to $Bi_2O_3 \cdot 2SO_3$ should correspond to the d-spacing of the pure solids. This has been verified for several fractional extents of decomposition of $Bi_2O_3 \cdot 3SO_3$ at 733 K. The same behavior has been observed for partial decomposition of $Bi_2O_3 \cdot 2SO_3$ to $Bi_2O_3 \cdot SO_3$ at 813 K.

The nature of the product of decomposition of $Bi_2O_3 \cdot SO_3$ is not as well defined:

$$Bi_2O_3 \cdot SO_3 = Bi_2O_3 \cdot nSO_3 + (1-n)SO_3 \ , n < 1 \ . \quad (10)$$

Most of the decompositions at 1048 K were carried to a composition close to $Bi_2O_3 \cdot (2/3)SO_3$. The diffraction patterns of the products are the same as those attributed by Matsuzaki et al.[12] to the above compositions. At 1240 K, the sharp break in reaction rate occurs at n = 0.30 rather than at n = 1/3. This corresponds more closely to the value of n = 0.30 claimed by Margulis et al.,[13] who also believe that a homogeneous solid exists between n = 0.30 and 0.40. Static pressure measurements and x-ray diffraction patterns as a function of mols of SO_3 removed probably are necessary to define a possible homogeneity range.

An approximate phase diagram[13] indicates that approximately 2.3 mols of SO_3 can evolve without the appearance of liquid if the temperature is kept below ~1250 K, an item of significant importance for process design.

B. Thermodynamics

Some equilibrium SO_3 pressures determined for the second stage of bismuth sulfate decomposition [reaction (8), above] are given in Table III and Fig. 11.

Extrapolation of these data (Fig. 3) shows that P_{SO_3} reaches 1-atm pressure at 1120 K. The derived enthalpy change for reaction (8) is 172.4 kJ/mol compared with an earlier experimentally determined value of 160.7 kJ/mol for reaction (7). These values refer to the temperature range of the measurements.

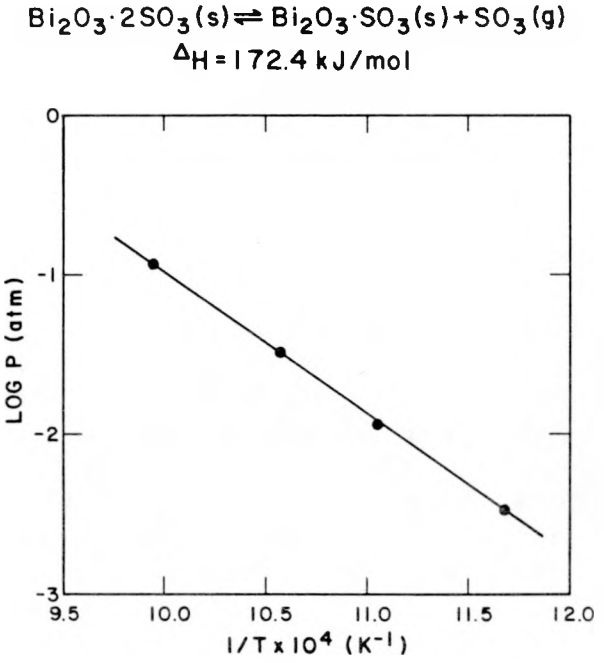

Fig. 11.
Equilibrium pressure measurements for bismuth oxysulfate decomposition.

C. Crystal Structure

The crystal form of the $Bi_2O_3 \cdot 2SO_3$ involved in the above equilibria is the high-temperature or β form, which we identified through its powder x-ray diffraction pattern. X-ray diffraction patterns of samples quenched after annealing at different temperatures for various times show that the transition temperature is between 800 and 825 K, but probably closer to 800 K.

The transformation is slow in the transition temperature range and may require >1000 h. However, the α form converts to the β form in <1 h at 885 K. In a year at room temperature, samples of β showed no tendency to transform to stable α. The transformation rates are valuable in planning equilibrium pressure measurements so as to ensure the presence of the known β form of $Bi_2O_3 \cdot 2SO_3$.

An additional crystal structure, α', has been observed for $Bi_2O_3 \cdot 2SO_3$ when formed from the reaction of Bi_2O_3 with either 1*M* or 4*M* H_2SO_4. The α' transforms to the α form of Bi_2O_3 at temperatures as low as 545 K. The α' form may be metastable, as no transformation of α' to α has been observed. The existence of either the α' or β form of $Bi_2O_3 \cdot 2SO_3$ probably will not significantly affect the process design or the efficiency of the LASL bismuth sulfate cycle.

TABLE III

EQUILIBRIUM PRESSURES FOR $Bi_2O_3 \cdot 2SO_3$ COMPOSITION

T(K)	$1/T \times 10^{-4}$	P_{total} (atm)	P_{SO_3} (atm)
856	11.7	1.11×10^{-2}	3.34×10^{-3}
905	11.1	4.08×10^{-2}	1.15×10^{-2}
946	10.6	1.15×10^{-1}	3.20×10^{-2}
1005	9.95	4.37×10^{-1}	1.18×10^{-1}

D. Bismuth Sulfate Decomposition Facility

A facility for studying continuous $Bi_2O_3 \cdot 2SO_3$ decomposition is to be built at LASL. At present, we plan to carry out the decomposition reactions in a fluidized-bed reactor with continuous feed and withdrawal of solid material. Initially, an inert gas such as nitrogen would be used as the fluidizing medium. Later we plan to switch to a gas mixture containing SO_2 and O_2 and promote the chemical heat-pipe mechanism to transfer heat to decompose the solid oxysulfate. The reactions involved in the decomposition take the form:

$$Bi_2O_3 \cdot 2SO_3 = Bi_2O_3 \cdot SO_3 + SO_3 \qquad (8)$$

$$Bi_2O_3 \cdot 2SO_3 = Bi_2O_3 \cdot (2/3)SO_3 + 1.33\ SO_3 \ . \qquad (11)$$

Drying methods and crystal structure are being studied before a final decomposition scheme is determined.

The compound $Bi_2O_3 \cdot 2SO_3$ was prepared in < 50-g batches at room temperature by using stoichiometric amounts of 1*M* H_2SO_4 and Bi_2O_3 starting material as well as excess amounts of either component. The resulting solid product was always composed of small needle-like particles that were 5-10 μ long and <1 μ in diameter. The particles agglomerated into spherical pills 70-100 μ in diameter. The $Bi_2O_3 \cdot 2SO_3$ material is white and thus is distinct from the yellow Bi_2O_3 reactant.

On precipitation at room temperature, the cake that formed after centrifugation contained 50-57 wt% solids in 0.2-0.4*M* H_2SO_4. Drying at 410 K in a vacuum oven removed most of the water, but heating at 575-625 K was necessary to drive off the final H_2SO_4 adhering to the solid precipitate. As the H_2SO_4 is concentrated by heating, reaction with $Bi_2O_3 \cdot 2SO_3$ occurs, forming some normal bismuth sulfate, $Bi_2O_3 \cdot 3SO_3$. X-ray patterns of the dried product show that most of it was $Bi_2O_3 \cdot 2SO_3$, but extra unaccounted-for lines were observed and these probably resulted from the above transformation.

A tubular quartz assembly has been set up to examine the feasibility of fluidizing the $Bi_2O_3 \cdot 2SO_3$ particles as they decompose. The powder is supported on a frit at the bottom of a cylindrical tube. A conical section joins the frit to the uniform section of the tube. These portions of the tube are encased in a muffle furnace, as shown in Fig. 12. Nitrogen gas is the fluidizing medium. After passage through the tube, the gases are bubbled through water for SO_3 absorption.

In the first test, pilling of the $Bi_2O_3 \cdot 2SO_3$ was a problem. The finely divided particles clumped into larger entities that did not fluidize and led to bed-channeling. The evolution of SO_3 between 775 and 1075 K was deduced from the fact that H_2SO_4 mist was detected in the gases leaving the water absorber. The final bed temperature was 1195 K.

After being cooled, the material was identified by x-ray analyses as $Bi_2O_3 \cdot (2/3)SO_3$ (as expected), with a possible small amount of $Bi_2O_3 \cdot 0.4SO_3$. In addition, some molten Bi_2O_3 collected on the tube walls a short distance above the top of the bed of particles.

We made two other unsuccessful attempts to maintain a fluidized bed. In the first attempt, dried

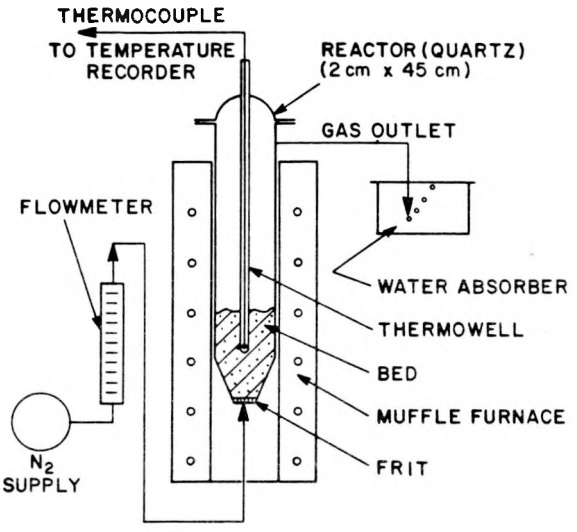

Fig. 12.
Schematic of fluidization apparatus for $Bi_2SO_3 \cdot 2SO_3$ decomposition.

powdery $Bi_2O_3 \cdot 2SO_3$ was added to the tube in which nitrogen was flowing. Pilling seemed to accelerate. In the second attempt, this procedure was tried in the tube at 875 K in the hope that decomposition might offset the pilling tendency.

One other approach to be tried is to compact the dried $Bi_2O_3 \cdot 2SO_3$ material by pressing it into pellets and to grind the compact into a size range of particles that may prove more favorable for fluidization. There is also the possibility of digesting the precipitated $Bi_2O_3 \cdot 2SO_3$ to allow growth of the particles, an approach that might also lessen the amount of liquid occluded with the solids and make filtration or centrifugation (to remove moisture) easier.

X. HI ELECTROLYSIS

We designed and built a cell to study electrolysis of HI and HI_5 at temperatures where the resulting iodine will remain liquid. It will operate at ~390 K, as the melting point of I_2 in HI is 385.3 K. This will be below the boiling point of HI (azeotropic 57% HI boils at 400 K).

The cell body is made of Teflon blocks. Electrodes were machined from graphite, with grooves cut parallel to the direction of electrolyte flow. The two

electrolytes, 57% HI and HI_5, are fed countercurrently by gravity to the inclined cell; the HI_5 flows downward to effect removal of liquid I_2, which is expected to flow along the grooves in the anode and leave the upper surfaces unobstructed. Hydrogen gas will move upward along the grooves in the cathode above.

The cell has been heated to 365 K in a water bath. A diaphragm of asbestos paper supported between pieces of glass cloth successfully prevented mixing of water solutions and will be tried with the actual electrolytes at 390 K. Electrolyte leaked through the pores of the graphite electrodes and seeped out around the tantalum leads, but this leakage was remedied by sealing the back of the electrodes with epoxy cement and coating the leads with glyptal.

The tendency of Teflon to creep at higher temperatures was a major problem. The seals of the cell depend upon pressure exerted upon the Teflon sandwich by bolted stainless steel flanges. These flanges were tightened at room temperature, but at the higher bath temperatures the flow of the Teflon loosened them. When more pressure was applied, the holes through which the glass tubing was inserted distorted sufficiently to crack the glass. Heavy-walled Teflon tubing used as connectors between the cell and the glass coils and outlets not only solved the problem but also served as shock absorbers and flexible joints between the cell and the glassware.

An experiment was conducted at 390 K with 55% HI as the catholyte and HI_2 as the anolyte, both flowing in a countercurrent mode. Grooved graphite electrodes were used, the cathode having been platinized. An asbestos diaphragm supported in a sandwich of glass cloth separated the two compartments. Shortly after the experiment started the two electrolytes were mixing considerably, even at flows of 3 ℓ/h. The asbestos diaphragm had torn, allowing the electrolytes to mix.

Electrolysis voltages in all experiments were higher than those required for a promising electrochemical step, and the study was discontinued.

XI. CONCLUSIONS AND PROGRAM PROJECTIONS

We plan to do a complete conceptual process design for a given thermochemical cycle. In the design, energy and mass flows will be computed to obtain a better estimate of cycle efficiency and cost. We intend to use these data for estimating the cost of fusion-based synfuel (hydrogen).

Our objectives also include the study of the continuous decomposition and recycle of solid compounds for use in thermochemical cycles. We plan to continue experiments with the "solids decomposition facility" that will include the development of a rotary kiln. Later we will study the $SO_2/O_2/SO_3$ chemical heat-pipe mechanism for heat transfer to solids. Kinetic and thermodynamic investigations will be carried out to obtain reaction rate and yield data as well as heats of reaction for solid compounds of interest in thermochemical cycles.

Technical information exchange activities will be coordinated primarily through IEA workshops on hydrogen production technology. The usual channels of publications and presentations also will be pursued.

Interesting thermochemical cycles being developed at other laboratories throughout the world will be evaluated for their technical feasibility and efficiency for DOE. Also, we will lend support to the DOE Thermochemical Cycle Evaluation Panel that is currently reviewing cycles under STOR sponsorship.

REFERENCES

1. K. E. Cox, "Thermochemical Processes for Hydrogen Production, March 1—September 30, 1978," Los Alamos Scientific Laboratory report LA-7629-PR (February 1978).

2. G. H. Farbman, "The Westinghouse Sulfur Cycle Hydrogen Production Process: Program Status," in *Hydrogen Energy System*, T. N. Veziroglu and W. Seifritz, Eds., Proc. 2nd World Hydrogen Energy Conf., Zurich, Switzerland, August 21-24, 1978.

3. J. D. de Graaf, K. H. McCorkle, J. H. Norman, R. Sharp, G. B. Webb, and T. Ohno, "Engineering and Bench-Scale Studies on the General Atomic Sulfur-Iodine Thermochemical Water-Splitting Cycle," in *Hydrogen Energy System*, T. N. Veziroglu and W. Seifritz, Eds., Proc. 2nd World Hydrogen Energy Conf. 2, 545-567, Zurich, Switzerland, August 21-24, 1978.

4. D. van Velzen, H. Langenkamp, G. Schutz, D. Lalande, J. Flamm, and P. Fiebelmann, "Development, Design, and Operation of a Continuous Laboratory-Scale Plant for Hydrogen Production by the Mark-13 Cycle," in *Hydrogen Energy System*, T. N. Veziroglu and W. Seifritz, Eds., Proc. 2nd World Hydrogen Energy Conf. **2**, 649-665, Zurich, Switzerland, August 21-24, 1978.

5. G. G. Urazov, P. S. Kindiakov, and A. K. Chukan, "Solubility in the Ternary System Bismuth Oxide-Sulfur Trioxide-Water at 25°C," Tr. Mosk. Inst. Tonkoi Khim. Tekh. **7**, 144-148 (1958).

6. M. G. Bowman and E. I. Onstott, "Hydrogen Production by Low Voltage Electrolysis in Combined Thermochemical and Electrochemical Cycle," Proc. Electrochem. Soc. Meeting, New York City, October 1974.

7. I. Barin, O. Knacke, and O. Kubaschewski, *Thermochemical Properties of Inorganic Substances* (Springer-Verlag, New York, 1977).

8. L. A. Booth, M. G. Bowman, G. E. Cort, K. E. Cox, D. J. Dudziak, J. H. Pendergrass, and A. S. Tai, "Production of Electrothermochemical Hydrogen Using a Fusion Source of High-Temperature Process Heat," Proc. 3rd ANS Topical Meeting on the Technology of Controlled Nuclear Fusion **1**, 180-192, Santa Fe, New Mexico, May 9-11, 1978.

9. *JANAF Thermochemical Tables*, 2nd Ed., Report NSRDS-NBS 37, Washington, D.C., 1971.

10. R. W. Dornte and C. V. Ferguson, "Solubility of Nitrogen and Oxygen in Liquid Sulfur Dioxide," Ind. Eng. Chem. **31**, 112-113 (1939).

11. Chem. Eng. **86**, 105 (March 26, 1979).

12. R. Matsuzaki, A. Sofue, H. Masumizu, and Y. Saeki, "Thermal Decomposition Process of $Bi_2(SO_4)_3$," Chem. Lett. (Japan) **7**, 737 (1974).

13. E. V. Margulis, N. S. Grishankina, and N. I. Kopylov, "Thermal Decomposition of Bismuth Sulfate," J. Inorg. Chem. USSR **10**, 1253 (1965).

☆ U.S. Government Printing Office: 1979 -- 677—013/184